Available online at www.sciencedirect.com
ScienceDirect
Wave Motion 43 (2006) 689–699
WAVE MOTION
www.elsevier.com/locate/wavemoti

Subharmonic generation in physical systems: An interaction-box approach

Federico Bosia [a,*], Nicola Pugno [b], Alberto Carpinteri [b]

[a] Department of Physics, Politecnico di Torino, Torino, Italy
[b] Department of Structural Engineering and Geotechnics, Politecnico di Torino, Torino, Italy

Received 1 February 2006; received in revised form 26 May 2006; accepted 1 June 2006
Available online 12 July 2006

Abstract

A so-called "interaction-box" formalism, which has recently been introduced to describe hysteresis in dynamical systems in the case of higher harmonic generation, is further discussed and generalized to describe the phenomenon of subharmonic generation. In this case, the increase in the periodicity of the response is reflected in the formation of multiple loops in the Effect (output) vs. Cause (input) diagrams. Conversely, we show how this type of response represents a sort of "signature" of the system, and can thus be employed to draw general conclusions about the features of the latter. A specific example of a nonlinear system is chosen to illustrate the approach, namely a vibrating cantilever beam with a breathing crack. Effect vs. Cause curves are calculated for this system in the presence of higher harmonics and subharmonics.

Keywords: Nonlinearity; Harmonic generation; NDE

1. Introduction

One of the most interesting findings in material science of recent years is that nonlinear hysteretic behaviour appears to be the norm rather than the exception [1] although in many practical situations a nonhysteretic and/or linear approximation may represent a very convenient and accurate description. In fact this seems to be the case in a wide variety of examples drawn from physics, biology, medicine or even sociological sciences [2–5]. Therefore, it is reasonable to attempt the development of a formalism as general as possible to describe this type of behaviour and capture its defining properties, and to apply it to specific examples with additional assumptions if needed. Such a formalism has been recently developed to describe the generation of higher harmonics by means of an "interaction-box" [6], which is used to model a system in a totally general fashion. In fact, one starts by assuming only that an unspecified Cause (the input) interacts with the system being considered (the box), yielding a certain Effect (the output), regardless of the nature of the system, of the input and of the output. More specifically, in Ref. [6] a monochromatic sinusoidal input is considered

* Corresponding author. Tel.: +39 0115647367.
E-mail address: federico.bosia@polito.it (F. Bosia).

0165-2125/$ - see front matter
doi:10.1016/j.wavemoti.2006.06.003

and a Fourier expansion of the output performed, thus generating higher harmonics of the driving frequency. The output vs. input curves are reminiscent of those obtained in Lissajou figures, thus showing how a hysteretic behaviour can be seen to derive in general from such simple assumptions, and that the entity of the hysteresis depends only on the phase shifts associated with the various harmonic components in the expansion. Here, the term "hysteresis" is used in its most general sense, indicating the lagging of a generic Effect behind its Cause.

In this contribution, we show that such a formalism can be generalized in order to describe generation of subharmonics as well as higher harmonics. The former differ considerably from the latter, since they have been seen to arise only above a certain excitation threshold [7–10]. This behaviour can be found in various different systems, ranging from acoustic wave interactions with cracked defects in solids [10], to the transfer of vibrations from a sample to the cantilever of an atomic force microscope [11]. Such systems display both higher harmonic and subharmonic generation, the latter with threshold amplitude behaviour as a function of the input excitation. This mechanism may also be introduced in our formalism, as we show in this paper, where the predictions are compared to those determined for the specific system of a vibrating cantilever beam with a breathing crack.

The paper is organized as follows: in Section 2, the interaction-box formalism is presented and extended to include subharmonic generation; in Section 3, the cantilever beam problem is presented, results are discussed and compared to those predicted by the interaction-box approach.

2. Including subharmonics in the interaction-box formalism

Without even the need of specifying the field of application or the nature of the input, let us assume that the cause is a sinusoidal signal $C = A\sin\omega t$, where A is its amplitude, ω its circular frequency and t the time. Generalizing the formalism of Ref. [6], we assume here that due to interaction with the "box" after the disappearance of any transient phenomena, the output will be given by

$$E(C(t)) = E_0 + \sum_{m,n=1}^{\infty} E_{mn}\sin\left(\frac{n}{m}\omega t + \varphi_{mn}\right). \tag{1}$$

Both higher harmonic and subharmonic components are present in the expansion, with amplitudes E_{mn} and phases φ_{mn}. When restricting the subharmonic generation to the order 1/2, i.e., $m = 1$, 2 only, and setting $E_{1n} = E_n$, $E_{2n} = E_{n-1/2}$, $\varphi_{1n} = \varphi_n$, and $\varphi_{2n} = \varphi_{n-1/2}$, Eq. (1) becomes

$$E(C(t)) = E_0 + \sum_{n=1}^{\infty} E_n\sin(n\omega t + \varphi_n) + \sum_{n=1}^{\infty} E_{n-1/2}\sin\left[\left(n-\frac{1}{2}\right)\omega t + \varphi_{n-1/2}\right]. \tag{2}$$

Here, as in Ref. [6], C and E can be any relevant quantities characterizing the system, e.g., load and displacement, or stress and strain. To account for the subharmonic threshold behaviour, the condition $E_{n-1/2} = 0$ if $E_1 < Q$ may be added, where Q represents the threshold in the input. In general, Q is expected to be a function of the driving amplitude and frequency [12]. A complete cycle of the cause occurs for $(2k-1/2)\pi \leqslant \omega t < (2k+3/2)\pi$, with k integer, whereas a complete cycle of the output occurs for $(2k-1/2)\pi \leqslant \omega t < [(2k+1)+5/2]\pi$, i.e., the generation of subharmonics of order 1/2 doubles the period of the output.

In accordance with the procedure adopted in [6], we rewrite the Effect $E(C(t))$ as a function of the normalized input $x = C/A = \sin\omega t = \sin\tau$, and $\cos\tau = \pm\sqrt{1-x^2}$. Consequently, for subharmonic oscillations

$$\sin\frac{\omega t}{2} = \pm\sqrt{\frac{1\mp\sqrt{1-x^2}}{2}} \qquad \cos\frac{\omega t}{2} = \pm\sqrt{\frac{1\pm\sqrt{1-x^2}}{2}} \tag{3}$$

and similarly for $\sin 3\omega t/2$, $\cos 3\omega t/2$ etc. Here, the $\pm$ signs are valid depending on the specific value of t considered in the cycle. In the case of harmonic generation, it is convenient to subtract the average value E_{av} of the output during a whole cycle from the output itself, and the resulting quantity can be rewritten as

$$\Delta E(x) = E(x) - E_{\mathrm{av}}(x) = G(x) \pm H(x), \tag{4}$$

where

$$G(x) = \sum_{n=1}^{N} \sum_{i=n}^{N} \gamma_{ni} P_i x^n \quad \text{and} \quad H(x) = \sqrt{1-x^2} \tag{5}$$

with $P_n = E_n \cos\varphi_n$, $Q_n = E_n \sin\varphi_n$ if n is odd; $P_n = E_n \sin\varphi_n$, $Q_n = E_n \cos\varphi_n$ if n is even and γ_{ni} and η_{ni} are numerical coefficients that vanish if i has a different parity from n. In particular, for the first five harmonics ($N = 5$) we have [6]

$$\gamma_{ni} = \begin{pmatrix} 1 & 0 & 3 & 0 & 5 \\ 0 & -2 & 0 & -8 & 0 \\ 0 & 0 & -4 & 0 & -20 \\ 0 & 0 & 0 & 8 & 0 \\ 0 & 0 & 0 & 0 & 16 \end{pmatrix} \qquad \eta_{\mathrm{ni}} = \begin{pmatrix} 1 & 0 & 1 & 0 & 1 \\ 0 & -2 & 0 & 4 & 0 \\ 0 & 0 & -4 & 0 & -12 \\ 0 & 0 & 0 & -8 & 0 \\ 0 & 0 & 0 & 0 & 16 \end{pmatrix} \tag{6}$$

When both higher harmonics and subharmonics of order 1/2 are present, the calculations are rather more cumbersome (and are omitted here for brevity), and the output can be expressed as $\Delta E = G \pm H \pm I \pm J + K^+(K^-) + L^+(L^-)$, where

$$I(x) = \sqrt{\frac{1 \pm \sqrt{1-x^2}}{2}} \sum_{n=1}^{N'} \sum_{i=n}^{N'} \kappa_{ni} R_i x^{n-1} \tag{7}$$

$$J(x) = \sqrt{\frac{1 \mp \sqrt{1-x^2}}{2}} \sum_{n=1}^{N'} \sum_{i=n}^{N'} \kappa_{ni} S_i x^{n-1} \tag{8}$$

$$K^+(x) = \sqrt{\frac{(1-x^2)(1+\sqrt{1-x^2})}{2}} \sum_{n=1}^{N'} \sum_{i=n}^{N'} \lambda_{ni} S_i x^{n-1} \tag{9}$$

$$K^-(x) = -\sqrt{\frac{(1-x^2)(1-\sqrt{1-x^2})}{2}} \sum_{n=1}^{N'} \sum_{i=n}^{N'} \lambda_{ni} S_i x^{n-1} \tag{10}$$

$$L^+(x) = \sqrt{\frac{(1-x^2)(1-\sqrt{1-x^2})}{2}} \sum_{n=1}^{N'} \sum_{i=n}^{N'} \lambda_{ni} R_i x^{n-1} \tag{11}$$

$$L^-(x) = -\sqrt{\frac{(1-x^2)(1+\sqrt{1-x^2})}{2}} \sum_{n=1}^{N'} \sum_{i=n}^{N'} \lambda_{ni} R_i x^{n-1} \tag{12}$$

with $R_i = E_{i-1/2} \sin\varphi_{i-1/2}$, $S_i = E_{i-1/2} \cos\varphi_{i-1/2}$ if i is even; $R_i = E_{i-1/2} \cos\varphi_{i-1/2}$, $S_i = E_{i-1/2} \sin\varphi_{i-1/2}$ if i is odd. Here, the appropriate $\pm$ signs must once again be/chosen according to the ωt value considered, and λ_{ni} and κ_{ni} are numerical coefficients that vanish when i has a different parity from n. For example, if only the first three subharmonics of order 1/2 are present ($N' = 3$), we have

$$\kappa_{ij} = \begin{pmatrix} 1 & 0 & 1 \\ 0 & 1 & 0 \\ 0 & 0 & -2 \end{pmatrix} \qquad \lambda_{ij} = \begin{pmatrix} 0 & 1 & 0 \\ 0 & 0 & 2 \\ 0 & 0 & 0 \end{pmatrix} \tag{13}$$

An important conclusion of these calculations is that in general four values of ΔE exist for any given value of x when 1/2-order subharmonics are present, vs. two values of ΔE in the case $m = 1$ (only higher harmonics), i.e., we obtain two hysteresis loops instead of one. Clearly, this is because when subharmonics are present in the system response, the output contains a smaller frequency than the input, and therefore the multiplicity of ΔE vs. x is in all cases greater than one, even when no hysteresis is present.

Figs. 1–3 depict the behaviour of $\Delta E(t)$ vs. the rescaled time $\tau = \omega t + \varphi$, and the Lissajou-type plots of $\Delta E(t)$ vs. $C(t)$ (i.e., the response of the system), for a generic nonlinear viscoelastic system such as that

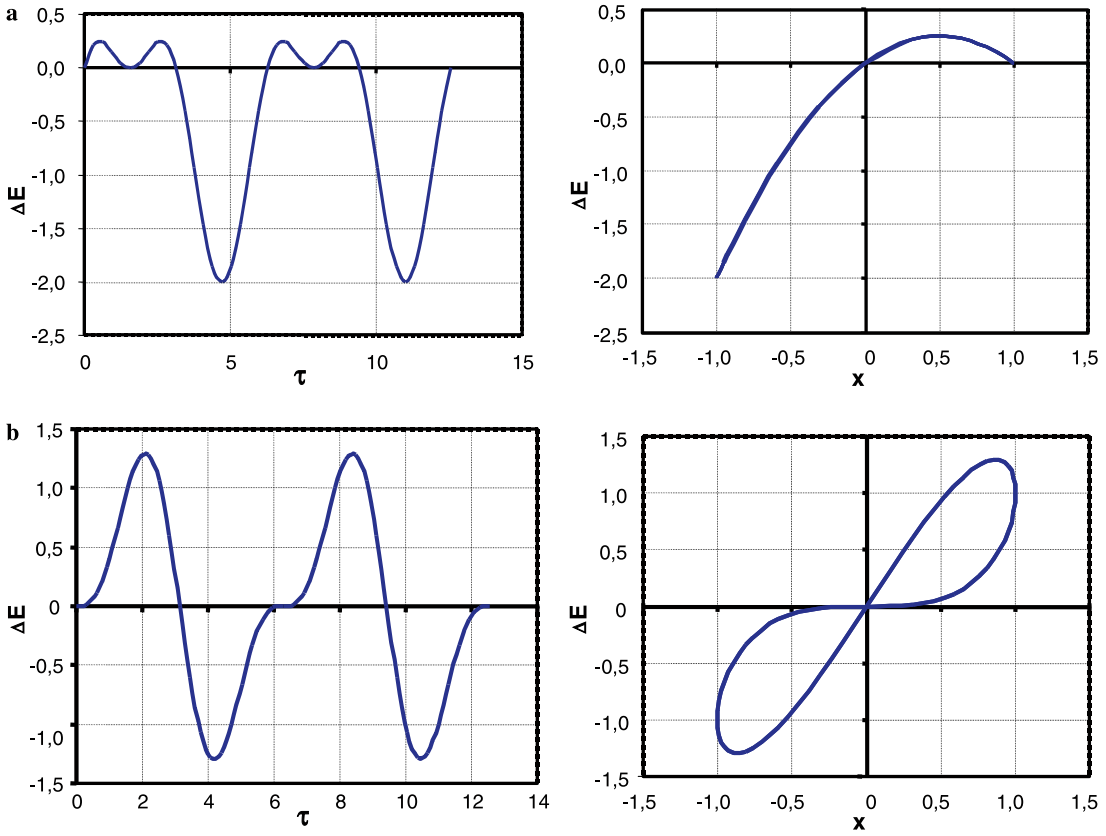

Fig. 1. Examples of the output ΔE of an interaction-box with respect to the rescaled time τ and the normalized sinusoidal input $x = C/A$ when only the second harmonic (E_2) is present in addition to the fundamental one (E_1). (a) $E_1 = 1$, $E_2 = 0.5$, $\varphi_1 = 0$, $\varphi_2 = \pi/2$, no hysteresis (degeneracy); (b) $E_1 = 1$, $E_2 = 0.5$, $\varphi_1 = 0$, $\varphi_2 = \pi$, hysteresis present. Both ΔE and τ are in arbitrary units.

considered up to this point, in various instances. In Fig. 1, besides the fundamental frequency only the first higher harmonic component is present with a phase value entailing: (a) no hysteresis and (b) hysteresis, respectively. In the latter case, characteristic loops appear in the $\Delta E(C)$ graph, as already shown in [6]. In Fig. 2, where only the first 1/2-order subharmonic adds to the fundamental frequency with phase values entailing: (a) no hysteresis and (b) hysteresis, respectively, the doubling of the period can be observed. Fig. 3 shows a response containing both the first higher harmonic and the first subharmonic component: (a) without hysteresis, (b) with 1/2-order subharmonic hysteresis, and (c) with additional second harmonic hysteresis.

Some general remarks can be made about the system response graphs:

Clearly, due to the periodicity of the input and output signals, in all cases closed curves are obtained; when n higher harmonics are present, up to n closed loops can appear in the response, the number of which depends on the specific amplitudes and phase values of the harmonics.

When subharmonics of various orders are present, the graph is multiple valued with a multiplicity that is at most twice the ratio between the fundamental frequency and that of the lowest-order subharmonic (e.g., in the case of 1/2-order subharmonics, the multiplicity is at most 4).

The threshold behaviour linked to subharmonic generation can be visualized in an numerical/experimental situation by a sudden doubling of the multiplicity in the system response curves when the threshold is exceeded.

These features, though fairly evident, can be exploited to rapidly characterize a dynamical system from the analysis of simple "output vs. input" graphs. Clearly, when an increasing number of higher harmonic and subharmonic components are present, each having generic phase values, the system response graphs become

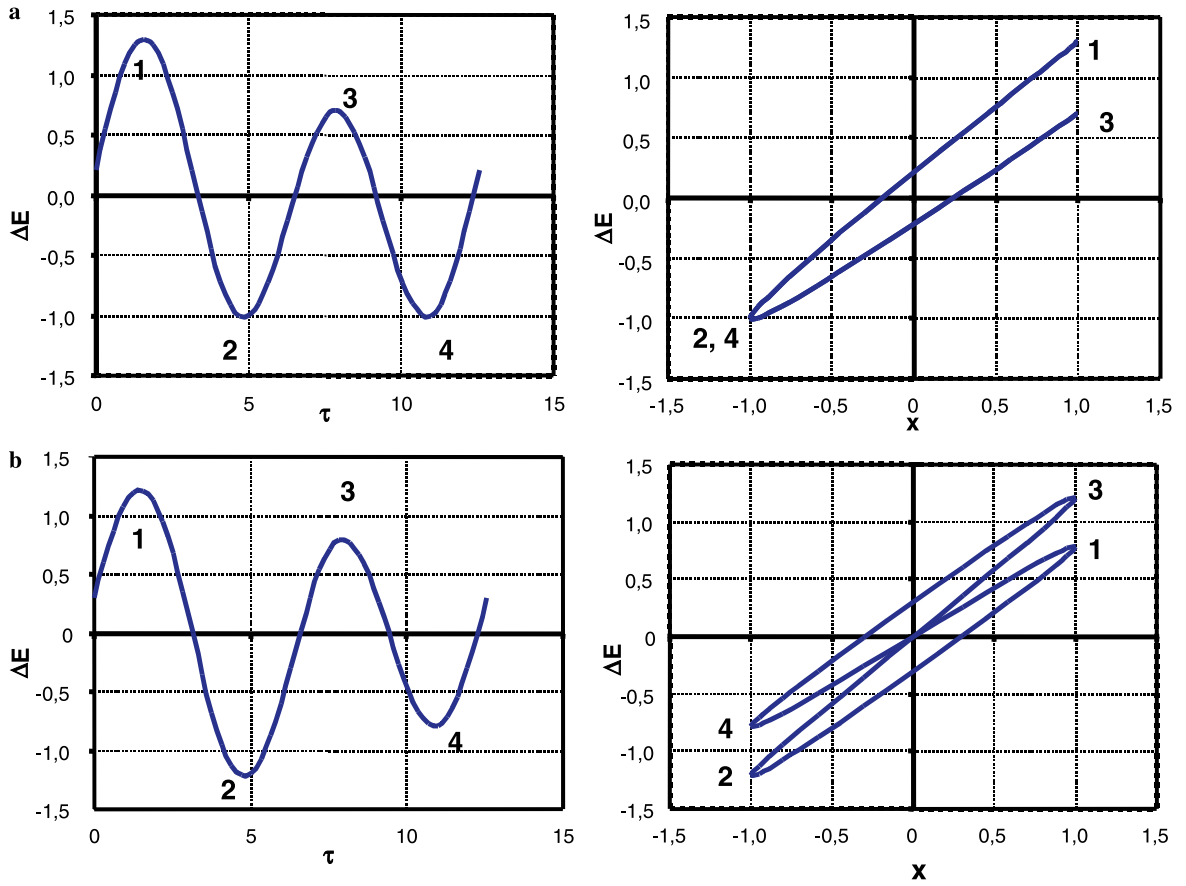

Fig. 2. Examples of the output ΔE of an interaction-box with respect the rescaled time τ and to the normalized sinusoidal input $x = C/A$ when only the first 1/2-order subharmonic is present. (a) $E_1 = 1$, $E_{1/2} = 0.3$, $\varphi_1 = 0$, $\varphi_{1/2} = \pi/4$, no hysteresis (degeneracy); (b) $E_1 = 1$, $E_{1/2} = 0.3$, $\varphi_1 = 0$, $\varphi_{1/2} = \pi$, hysteresis present. Corresponding points on associated graphs are indicated with increasing numbers (1 . . . 4).

more and more complex, until quasi-chaotic curves are obtained, and little can be said about the specific harmonic or subharmonic components present. One such example is given in Fig. 4, where five higher harmonics and three 1/2-order subharmonics are present.

3. Application of the formalism to a vibrating cantilever beam with a breathing crack

As a specific example of an application of our treatment, we consider a cracked cantilever beam clamped at one end and driven by a perpendicular sinusoidal force at the other. The crack "breathes", i.e., opens and closes continuously during vibration and thus causes a variation in the stiffness of the structure, and therefore a nonlinearity. Experimental studies on such a system [13] show that subharmonic generation (i.e., period doubling) is observed in the case of a strongly damaged structure.

The mathematical treatment adopted herein to predict the generation of higher harmonics and subharmonics is reported in detail in [14,15] and an extensive parametric study can be found in [16]. The approach is based on a discretization of the dynamic equilibrium beam equation using the finite element method. The stiffness of the cracked element is assumed to vary linearly with the element curvature between that of a fully open state and that of a fully closed state. The solution is assumed in the form of Eq. (1) with $m = 1 \ldots 4$, i.e., containing both higher harmonics and subharmonics of up to the fourth order, and the amplitudes of the components are determined using the harmonic balance method. The beam considered herein is similar to that described in the experimental analysis in [13], and is shown

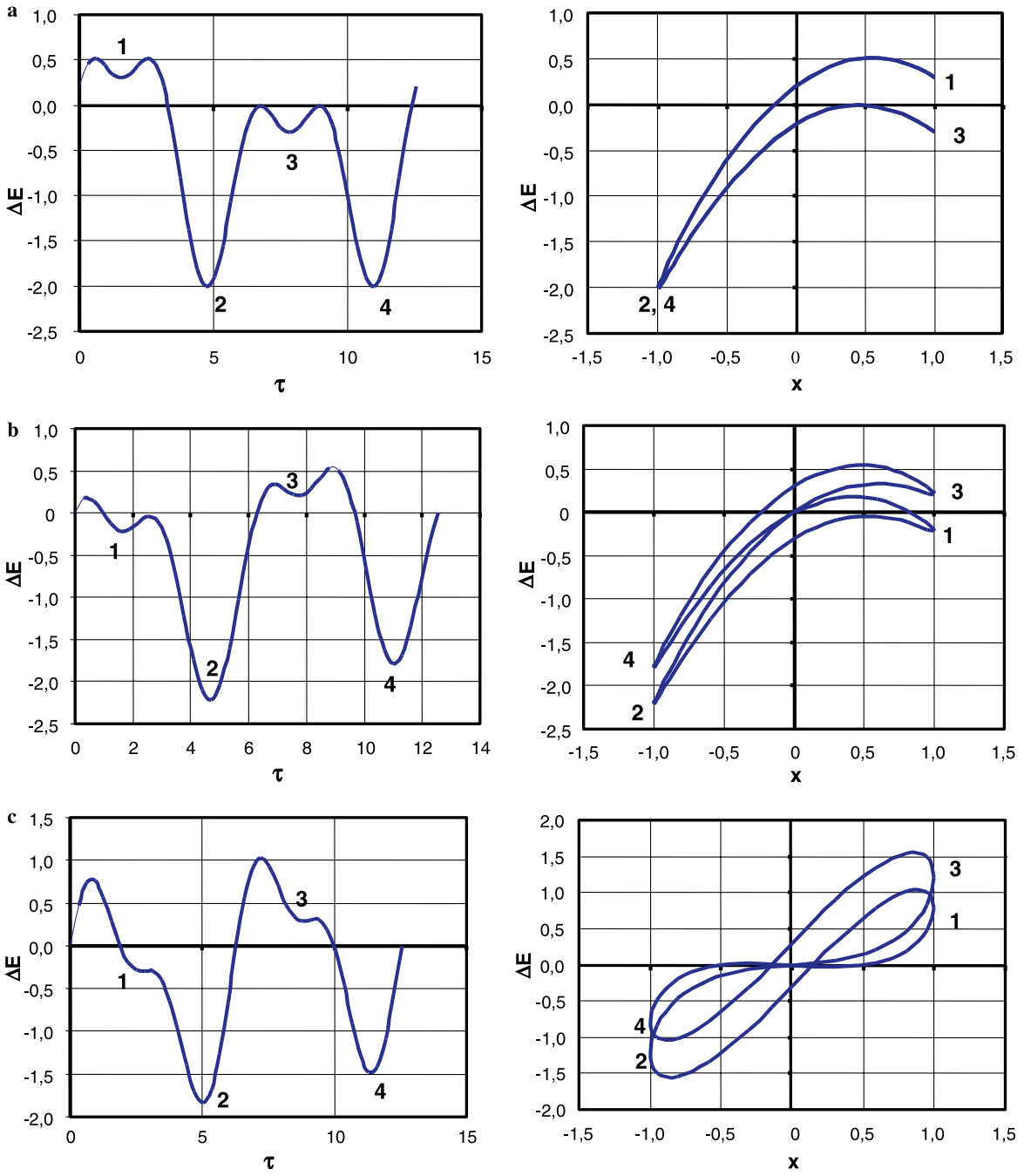

Fig. 3. Examples of the output ΔE of an interaction-box with respect to the rescaled time τ and the normalized sinusoidal input $x = C/A$ when both the first harmonic and 1/2-order subharmonic are present. (a) $E_1 = 1$, $E_2 = 0.5$, $E_{1/2} = 0.3$; $\varphi_1 = 0$, $\varphi_2 = \pi/2$, $\varphi_{1/2} = \pi/4$; (b) $E_1 = 1$, $E_2 = 0.5$, $E_{1/2} = 0.3$; $\varphi_1 = 0$, $\varphi_2 = \pi/2$, $\varphi_{1/2} = \pi$; (c) $E_1 = 1$, $E_2 = 0.5$, $E_{1/2} = 0.3$; $\varphi_1 = 0$, $\varphi_2 = \pi$, $\varphi_{1/2} = \pi$. No hysteresis (degeneracy) occurs only in case (a), when the phase of the subharmonic component assumes the appropriate value.

in Fig. 5. Its length is $l_1 = 230$ mm and its transversal square cross-section is $S = 400\ \text{mm}^2$; the specimen material is steel, with a Young's modulus of $Y = 2.06 \times 10^{11}\ \text{N/m}^2$, a density of $\rho = 7850\ \text{kg/m}^3$ and a modal damping coefficient of $\eta = 0.02$. A monochromatic Cause, i.e., a sinusoidal force applied at the tip, is considered. The Effect is chosen as the tip deflection. In the conventional Euler–Bernoulli approach,

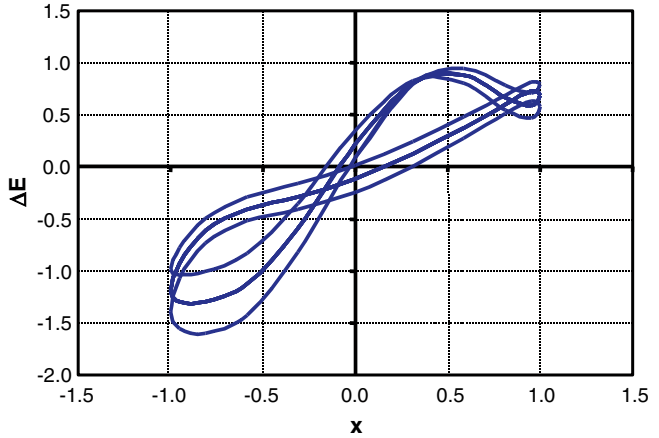

Fig. 4. Example of $\Delta E(x)$ when five harmonic and three 1/2-order subharmonic components are present: $E_1 = 1$, $E_2 = 0.3$, $E_3 = 0.2$, $E_4 = 0.1$, $E_5 = 0.05$, $E_{1/2} = 0.2$, $E_{3/2} = 0.1$, $E_{5/2} = 0.05$; $\varphi_1 = 0$, $\varphi_2 = \pi/6$, $\varphi_3 = \pi/3$, $\varphi_4 = 0$, $\varphi_5 = 0$, $\varphi_{1/2} = \pi/6$, $\varphi_{3/2} = \pi/10$, $\varphi_{5/2} = 0$.

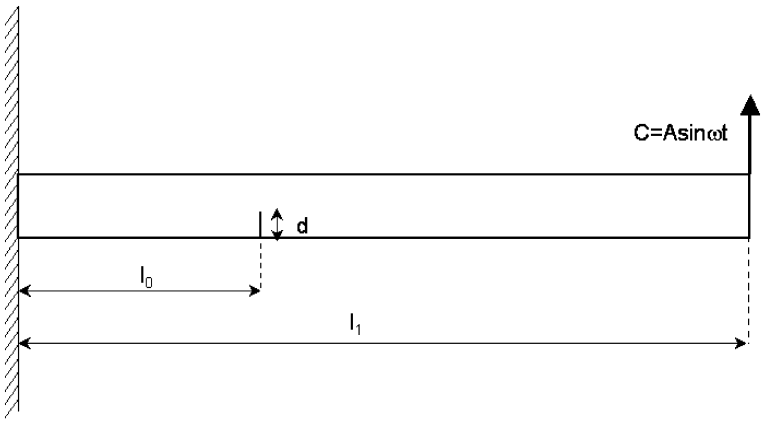

Fig. 5. Cantilever beam sample with a breathing crack of length d, forced by a sinusoidal Cause $C(t)$.

four boundary conditions must be imposed, i.e., zero deflection and first spatial derivative of the deflection at the clamped end, zero torque and a shear force (the sinusoidal Cause) applied at the free end. The crack is located in the specimen at one third of the total beam length, at a distance $l_0 = 77$ mm from the clamp, and is perpendicular to the longitudinal beam axis, as shown in Fig. 5. The nonlinearity can be increased by varying the crack depth d.

Simulations are performed using as in Section 2 a sinusoidal Cause $C = A \sin \omega t$ with amplitude $A = 10$ N and frequency $f = \omega/2\pi = 61$ Hz. The sample is discretized using 20 finite elements. The variation of the amplitudes of generated higher harmonics and subharmonics are computed for various values of the crack depth, for a constant driving amplitude.

Results for the growth of higher harmonic components and appearance of subharmonic components as a function of the crack depth d, i.e., the system nonlinearity, are reported in Fig. 6. The appearance of higher harmonics E_2, E_3 and E_4 and an offset E_0 (a zero frequency component, corresponding to the presence of a negative offset in the deflection of the free end) is observed even for a weak nonlinearity ($d < 30\%$) in Fig. 6a. The amplitudes of the fundamental vibration E_1 and of the second harmonic E_2 are the strongest components and remain virtually constant for increasing values of d; the offset E_0 increases for crack depth values of up to about $d = 35\%$, then levels off; the other two higher harmonic components initially grow, then decrease between $d = 35\%$ and $d = 50\%$ and $d = 60\%$, respectively, then begin to increase once more. The

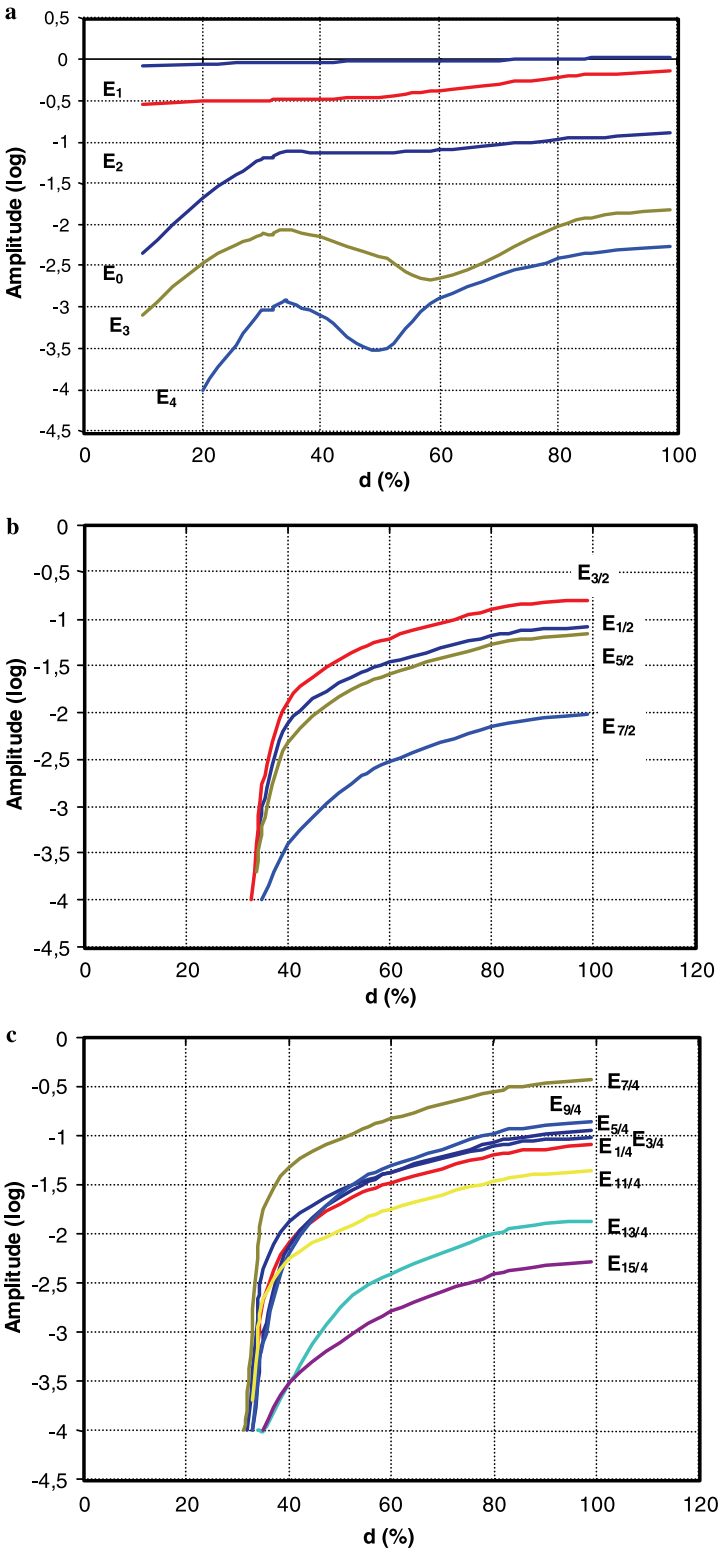

Fig. 6. Predicted amplitudes (in mm) for a sinusoidally excited cracked cantilever vs. crack depth d: (a) fundamental and higher harmonics; (b) 1/2-order subharmonics; (c) 1/4-order subharmonics.

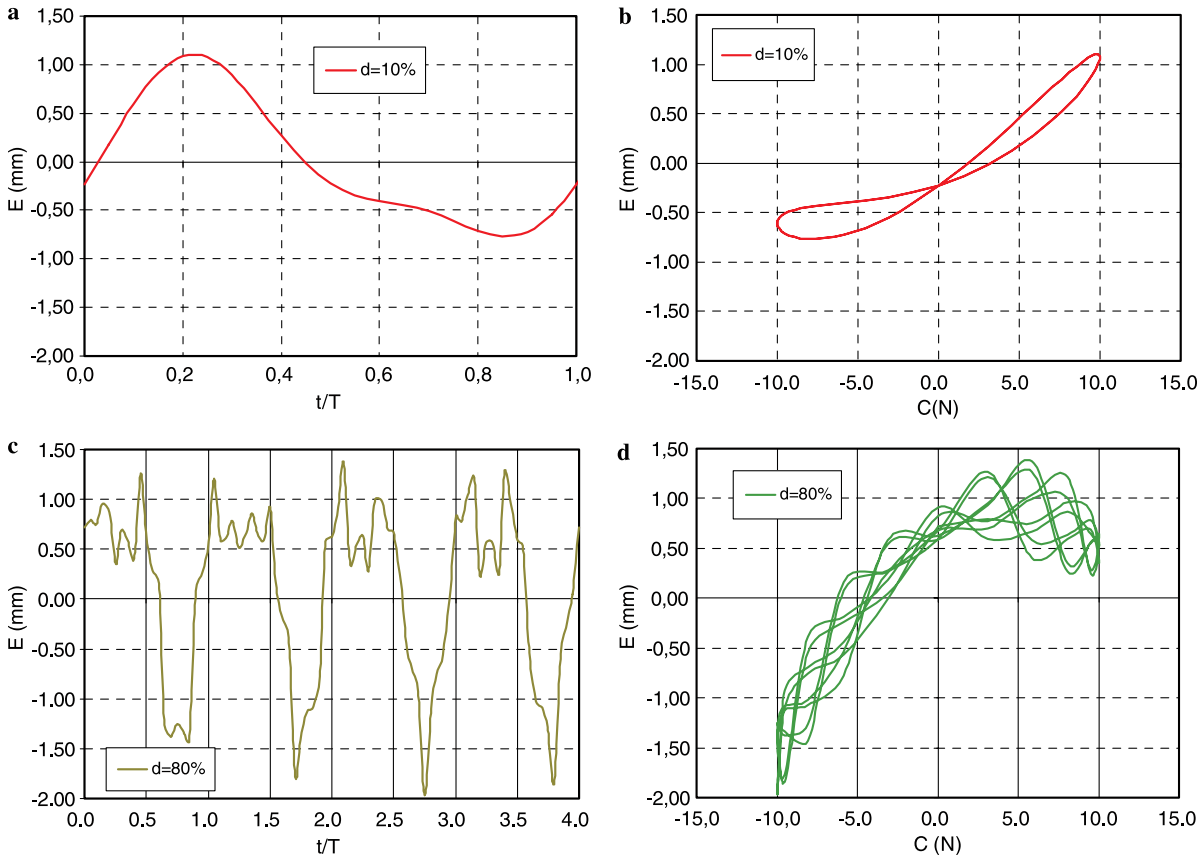

Fig. 7. Simulated results for a cracked cantilever beam excited sinusoidally, for two different crack depths d: (a) output E vs. time over two periods, $d = 10\%$; (b) output E vs. input C, $d = 10\%$; (c) output E vs. time over two periods, $d = 80\%$; (d) output E vs. input C, $d = 80\%$.

Table 1
Generated higher harmonic and subharmonic amplitudes E_n (in mm) and phases φ_n for two different percentage values of crack depth d in a cracked cantilever beam

n	0	1/4	1/2	3/4	1	5/4	3/2	7/4	2	9/4	5/2	11/4	3	13/4	7/2	15/4	4
$d = 10\%$																	
E_n	0.01				0.84				0.29				0.01				
φ_n					−0.01				−0.95				0.62				
$d = 80\%$																	
E_n	0.11	0.06	0.07	0.08	1.01	0.09	0.13	0.29	0.59	0.11	0.05	0.03	0.01	0.01	0.01	0.01	0.01
φ_n		−1.21	−0.84	−0.48	−0.01	0.27	0.63	0.99	1.47	−1.39	−1.02	−0.64	−0.48	0.07	0.44	0.79	1.18

decrease in amplitudes is an indication that energy is being transferred to previously absent subharmonic vibration modes.

This observation is confirmed by results reported in Figs. 6b and c: subharmonic components emerge for above-threshold values of the nonlinearity, i.e., of the parameter d in this case. In the case of the particular specimen considered, we find that the first subharmonic to appear is the $7/4\omega$ component for $d = 31.4\%$, followed by a $3/4\omega$ component for $d = 32\%$. The first 1/2-order subharmonic appears for $d = 33\%$. It is interesting to notice how in this system the thresholds for the appearance of 1/2-order and 1/4-order subharmonics are practically coincident (Figs. 6b and c). The threshold values are consistent with the behaviour highlighted

in Fig. 6a, i.e., an initial decrease in higher harmonic amplitudes for above-threshold d values. Once the subharmonic modes are generated, they continue to grow in amplitude with increasing crack depth values.

Fig. 7 illustrates the system response $E(t)$ for two values of the crack depth d, one above and the other below the subharmonic generation threshold. The system Effect is plotted both as a function of time and as a function of the chosen sinusoidal Cause $C(t)$. The two cases are considered for a crack depth of $d = 10\%$, where only the fundamental frequency and the second and third harmonics are present, and for $d = 80\%$, where various subharmonic components are also present. The overall higher harmonic and subharmonic amplitudes E_n and phases φ_n in the two cases are reported in Table 1. It is interesting to observe how the increasing nonlinearity modifies the signal from a behaviour similar to that highlighted in Figs. 1–3, towards increasingly complex figures, as discussed in Section 2, indicating a significant amount of damage present in the considered beam. This can be an useful indicator of the state of integrity of this and other structures, i.e., the sudden transition from below to above the subharmonic threshold vibration can be easily detected by plotting Effect vs.Cause graphs, and taking the doubling of the number of solutions as a preliminary on/off signal of significant structural deterioration. Finally, for increasing crack lengths, the system tends towards an increasingly chaotic behaviour, and the analysis of the system response by means of Effect vs. Cause graphs loses its significance, as the contribution of the various frequencies becomes hard to discern.

4. Conclusions

In this paper, we have generalized the interaction-box formalism to describe subharmonic as well as higher harmonic generation in physical systems. We show how Output vs. Input graphs are modified by an increase in the periodicity of solutions, and how general conclusions may be derived from the simple analysis of such graphs. Indeed, both the nonlinear and the hysteretical properties of nonlinear systems are analysed in a straightforward, even visual manner, contrary to e.g., standard spectral analysis, where the hysteretical properties of the system are usually not considered. The proposed approach is totally general in its formulation, and can therefore be applied to systems where any number of harmonics and subharmonics is present. The predictions of the modified formalism has also been compared to a specific example, i.e., a vibrating cantilever beam with a breathing crack. It is known that in many cases subharmonic vibrations display a threshold behaviour for increasing forcing amplitudes; in this example, we show this threshold behaviour appears also for increasing system nonlinearity, i.e., for increasing values of the crack depth. Results highlight a similar threshold dependence for both 1/2-order and 1/4-order subharmonic components. The analysis of Effect vs. Cause graphs provides a simple tool for monitoring damage progression in vibrating structures. The appearance of subharmonic vibrations, i.e., a doubling of the multiplicity of the E vs. C curves can for example be taken as a preliminary on/off indication of the loss of structural integrity of components under test.

Acknowledgements

The authors thank Prof. P. P. Delsanto (Politecnico di Torino) for continuous support and Dr. S. Hirsekorn (IZFP, Saarbrücken) for fruitful discussions, and acknowledge support from EC (AERONEWS Grant No. FP6-502927) and from ESF (NATEMIS Grant).

References

[1] R.A. Guyer, P.A. Johnson, Nonlinear mesoscopic elasticity: evidence for a new class of materials, Phys. Today 52 (1999) 30.
[2] G. Bertotti, Hysteresis and Magnetism for Physicists, Material Scientists and Engineers, Academic Press, 1998.
[3] M. Scalerandi, G.P. Pescarmona, P.P. Delsanto, B. Capogrosso-Sansone, Phys. Rev. E 63 (2000) 1, 011901.
[4] G.C. Kember, G.A. Fenton, K. Collier, J.A. Armour, Phys. Rev. E 61 (2000) 1816.
[5] R. Cross, J. Darby, J. Ireland, L. Piscitelli, Hysteresis and Unemployment: a Preliminary Investigation'', in ''Computing in Economics and Finance'', N. 721 (1999); see also various contributions to the First SIAM-EMS Conference AMCW 01, Berlin, September 2001.
[6] S. Hirsekorn, P.P. Delsanto, On the universality of nonclassical nonlinear phenomena and their classification, Appl. Phys. Lett. 84 (2004).
[7] P.J. King, M. Luukkala, Subharmonic generation in quartz plates, J. Phys. D: Appl. Phys. 6 (1973) 1047–1051.

[8] A. Alippi, G. Shkerdin, A. Bettucci, F. Craciun, E. Molinari, A. Petri, Low-threshold subharmonic generation in composites structures with cantor-like code, Phys. Rev. Lett. 69 (1992) 3318–3321.
[9] S. Ostapenko, I. Tarasov, Nonlinear resonance ultrasonic vibrations in Czochralski-silicon wafers, Appl. Phys. Lett. 76 (16) (2000) 2217–2219.
[10] I.Y. Solodov, B.A. Korshak, Instability, chaos, and "memory" in acoustic-wave–crack interaction, Phys. Rev. Lett. 88 (1) (2002) 014303.
[11] N.A. Burnham, A.J. Kulik, G. Gremaud, Nanosubharmonics: the dynamics of small nonlinear contacts, Phys. Rev. Lett. 74 (25) (1995) 5092–5095.
[12] C. Hayashi, Nonlinear Oscillations in Physical Systems, Princeton University Press, Princeton, 1985.
[13] J.A. Brandon, C. Sudraud, An experimental investigation into the topological tability of a cracked cantilever beam, J. Sound Vibr. 211 (1998) 555–569.
[14] N. Pugno, R. Ruotolo, C. Surace, Evaluation of the non-linear dynamic response to harmonic excitation of a beam with several breathing cracks, Int. J. Sound Vibr. 235 (2000) 749–762.
[15] A. Carpinteri, N. Pugno, Towards chaos in vibrating damaged structures – Part 1: theory and period doubling cascade in print, J. Appl. Mech. (2005).
[16] A. Carpinteri, N. Pugno, Towards chaos in vibrating damaged structures – Part 2: parametrical investigation in print, J. Appl. Mech. (2005).